

A facile approach to hexagonal ZnO nanorod assembly

K. Uma · S. Ananthakumar · R. V. Mangalaraja ·
K. P. O. Mahesh · T. Soga · T. Jimbo

Received: 7 August 2008 / Accepted: 14 October 2008 / Published online: 4 November 2008
© Springer Science+Business Media, LLC 2008

Abstract Nanocrystalline ZnO nanorods were successfully grown by ultrasonication using an acidic ethanolic zinc acetate precursor solution followed by a flow coating process and annealing at 600 °C. The ZnO nanorods obtained were hexagonal in shape and showed a high degree of uniformity in size and distribution. These samples were characterized by X-ray diffraction (XRD), energy dispersive X-ray (EDX) spectroscopy, X-ray photoelectron spectroscopy (XPS), scanning electron microscopy (SEM) and Raman spectrophotometry and the results are discussed. This approach appears to be the easiest way to fabricate bulk ZnO nanorods.

Keywords ZnO · Nanorod · Ultrasonication · Flow coating process

1 Introduction

As one of the most important wide band gap semiconductors (3.3 eV at 298 K) with a large exciton binding energy, ZnO nanostructures have attracted a high degree of interest for the fabrication of various types of nano-devices [1, 2]. One dimensional ZnO structures are considered especially important due to their capability for providing low-dimensional electron confinement [3–5] which has a large scope in the design and construction of functional electronic devices in the application areas of sensing, field emission, photovoltaics and optoelectronics. ZnO nanocrystallites with controlled size, shape and specific orientation on the substrate surface are a prerequisite for achieving high performance when actually used in applications. Methods including chemical, electrochemical, physical and chemical vapour deposition have been reported for preparing oriented ZnO nanorods and nanowires. The synthesis has also been extended to hydrothermal [6], solvothermal [7], sol–gel [8], laser ablation [9], solution [10] and template-assisted growth techniques [11]. Other than these techniques, catalyst-assisted growth is also employed for bulk nanostructures [12]. However, it often suffers from the disadvantage of introducing metal catalysts at comparatively high temperatures, which makes the whole synthesis more complex. The metal catalyst may also introduce impurities in the end product which directly affects the semiconducting properties of the ZnO nanostructures. In recent years, with the rapid development of ultrasound technology in chemistry,

K. Uma
Centre for Social Contribution and Collaboration, Nagoya
Institute of Technology, Nagoya 466-8555, Japan
e-mail: umamahesh16@gmail.com

S. Ananthakumar
Materials and Minerals Division, National Institute for
Interdisciplinary Science and Technology (CSIR), Trivandrum
695019, Kerala, India

R. V. Mangalaraja
Department of Materials Engineering, University of Concepcion,
Concepcion, Chile

K. P. O. Mahesh
Department of Materials Science and Engineering, Nagoya
Institute of Technology, Nagoya 466-8555, Japan

T. Soga (✉)
Department of Frontier Materials, Nagoya Institute of
Technology, Nagoya 466-8555, Japan
e-mail: soga@nitech.ac.jp

T. Jimbo
Department of Environmental Technology and Urban Planning,
Nagoya Institute of Technology, Nagoya 466-8555, Japan

sonochemical methods are being suggested for preparing ZnO nanostructures under ambient conditions [13]. Many materials synthesis experts claim that in sonochemical techniques, the ultrasonic waves produce micro-bubble reactors with large amounts of energy available for any chemical reaction to occur. Generation of temperatures up to ~ 5000 K and pressures of approximately 1800 atmosphere is expected when the microbubbles collapse during ultrasonic cavitation [14, 15]. However, due to the extremely high cooling rates in excess of 10^{10} K/s by the surrounding bulk liquid, sonochemical synthesis can be exploited for ZnO nanostructures under normal temperature and pressure without any additional heating of the precursor mixture. Hence, this technique is fast, simple and convenient. In this work, we have attempted to adopt the ultrasonication method for obtaining ZnO nanorods. Zinc acetate as a precursor in an ethanol medium was employed and no surfactant or organic amine was used as reported in earlier works [16, 17]. To our knowledge, the synthesis of ZnO nanorods by simple ultrasonication of the precursor solution prepared in an acidic medium followed by flow-coating and thermal annealing has seldom been reported [18, 19].

2 Experimental

ZnO nanorod assembly was fabricated over Corning glass substrates having an area of $2\text{ cm} \times 2\text{ cm}$. The ultrasonic energy was generated by a laboratory ultrasonic cleaner (USK-2A, 100 V, 50–60 Hz, China). The equipment was fitted with transducers at the bottom and the ultrasonicator was powered by a generator with automatic tuning to the resonant frequency and 60 Hz wave modulation. A sonication frequency of 40 kHz was selected for the synthesis. The sonication energy was given for a total duration of 15 min in five steps with an interval of 20 s every 3 min. At this frequency, the thermal energy generated inside the reaction mixture was conveniently mild and therefore evaporation of the ethanol solvent was prevented. Also, under the given conditions, it was envisaged that the reactants would undergo a controlled rate of thermohydrolysis. Optimum conditions were reached by many trial experiments. In fact we observed that continuous ultrasonication induced only precipitation and segregation of zinc hydroxides.

Zinc acetate di-hydrate salt ($\text{Zn}(\text{CH}_3\text{COO})_2 \cdot 2\text{H}_2\text{O}$, Nacalai Tesque Chemical Co. Ltd., 99.5%) was used as the precursor for growing ZnO nanorods. Anhydrous ethanol (Hayashi pure chemical Co., Ltd., 99%) solvent was used to induce the hydrolysis reaction of zinc acetate di-hydrate and HCl acid (Hayashi pure chemical Ind., Co., Ltd.) was used to achieve controlled hydrolysis. The precursor

solution was maintained at a pH value of 3. In a typical synthesis 0.5 g of $\text{Zn}(\text{CH}_3\text{COO})_2 \cdot 2\text{H}_2\text{O}$ was dissolved in 10 mL of ethanol solvent. About 4 g of 10 wt.% HCl/ethanol solution was prepared and was added slowly to the $\text{Zn}(\text{CH}_3\text{COO})_2 \cdot 2\text{H}_2\text{O}$ /ethanol solution with sonication. The precursor solution became transparent after sonication for 10 min. The zinc acetate di-hydrate was completely miscible in acidified ethanol. From this parent solution several drops were deposited on the Corning glass surface at a constant rate. Before coating, the Corning (7059) glass substrates were ultrasonically cleaned for 10 min in acetone then in methanol and dried with nitrogen. The coated glass substrates were kept in an electrically preheated chamber at 300°C for 5 min and then the solution was deposited again. This procedure was repeated five times. Finally, the substrates were annealed at 600°C for 3 h in an air atmosphere at a rate of $20^\circ\text{C}/\text{min}$. A white layer of oxide coating was seen on the substrate surface after annealing. The morphology of the coating was observed by scanning electron microscopy (SEM, S-3000H Hitachi). The crystallinity of the ZnO coating was analyzed using an X-ray diffractometer (X-ray diffractometer—JEOL) with Cu K α radiation. The sample was also tested for X-ray photoelectron spectroscopy (X probe SSX-100). Raman spectra were recorded using a Raman spectrometer (NRS 1500W Raman Spectrometer—JASCO) with an excitation wavelength of 523 nm.

3 Results and discussion

The X-ray diffraction analysis of ZnO coated glass substrates in the deposited and annealed conditions is presented in Fig. 1. The diffraction pattern of un-annealed coatings shows broad and weak peaks that confirm the formation of ZnO nuclei even in the deposited condition. The X-ray pattern further shows that the peaks are semi-crystalline and become fully crystalline after annealing at 600°C (Fig. 1b). All the peaks belong to hexagonal bulk ZnO and the X-ray pattern matches well with the JCPDS card No. 89-1397. The high intensity and narrow spectral width of the ZnO peaks obtained in the XRD pattern suggest that the ZnO coating has good crystalline quality with (101), (100), and (002) lattice planes. It is also seen that the annealing temperature of 600°C is adequate for achieving well crystallized and oriented ZnO nanorods. When the deposited precursor coatings are subjected to 300°C , zinc acetate di-hydrate is probably decomposed and produces active primary ZnO nuclei which further acts as a seed layer. When the deposition is repeatedly performed, the freshly formed nuclei from the precursor solution have a tendency to lead the growth from the seed layer. Once the nuclei are formed, there are large numbers

of dangling bonds, defects, or traps on the nuclei surface and during annealing further nucleation and growth occurs in a specific pattern. In this experiment active zinc nuclei are formed by ultrasonication and well-defined, crystalline, hexagonal faces are grown on the glass surface by annealing at a temperature of 600 °C. The translucent ZnO coated glass substrates under deposited conditions become opaque after annealing.

SEM images of the ZnO coatings in (a) as grown and (b) annealed at 600 °C conditions are presented in Fig. 2. The deposited coatings exhibit only a layered microstructure (Fig. 2a). The layers became well crystallized randomly oriented hexagonal ZnO rods during annealing and Fig. 2b clearly shows the nanorod assembly. These nanorods have dimensions ranging from 400 to 500 nm and only a few rods showed sizes as large as 600 nm. However, this is the largest size obtained by this technique.

The stoichiometry of the samples was examined by the EDX spectrum as shown in Fig. 3. Only zinc and oxygen signals have been detected, suggesting that the nanorod is indeed made up of Zn and O. The Zn/O ratio is about 1.18, indicating an oxygen deficiency in the fabricated zinc oxide coatings. The results are further confirmed by the XPS analysis which is presented in Fig. 4. The major elements Zn and O with minor C peaks were detected from the XPS spectra.

The typical Raman spectrum of the ZnO nanorods is shown in Fig. 5. The spectrum shows an intense peak at 441 cm^{-1} . When it is compared with the bulk ZnO, there is a shift of 2 cm^{-1} . It corresponds to the E_2 mode of the wurtzite ZnO crystal. It further supports that the coatings consist of ZnO nanorods [20]. The peak at 330 cm^{-1} should be assigned to the second order Raman spectrum arising from zone-boundary phonons $3E_2H-E_2L$, while the dominant peak at 569 cm^{-1} is contributed by the E_1 (LO)

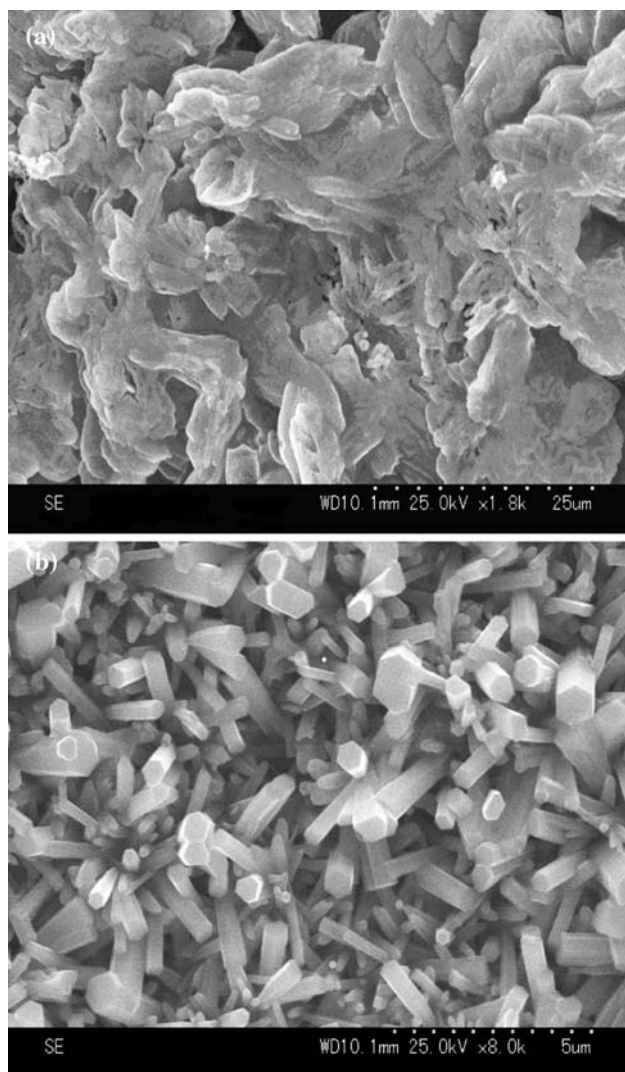


Fig. 2 SEM images of the Corning glass substrates **a** ZnO layers at 300 °C, **b** annealed coated layers at 600 °C

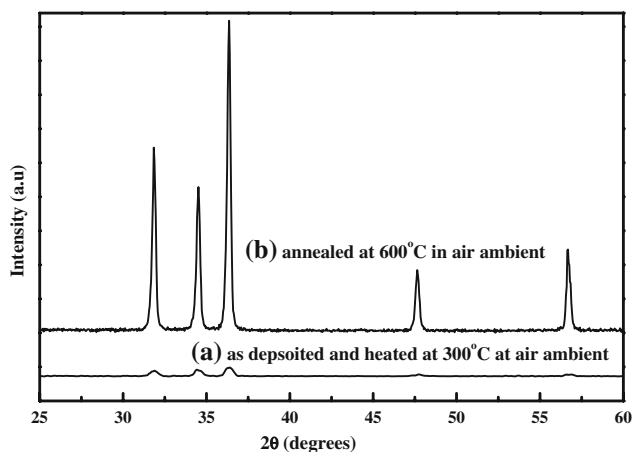


Fig. 1 XRD pattern of Corning glass substrates (a) as deposited and heated at 300 °C at air ambient, (b) substrates annealed at 600 °C in air ambient

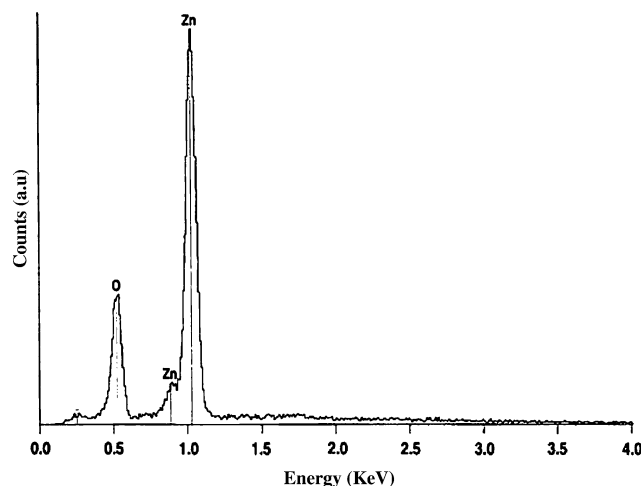


Fig. 3 EDX spectrum of ZnO nanorods deposited on Corning glass annealed at 600 °C in air ambient

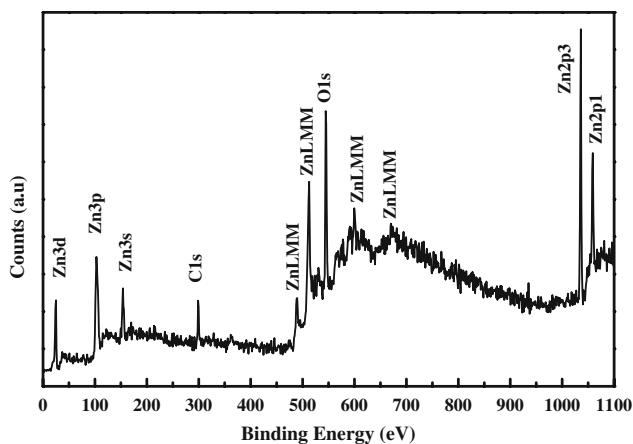


Fig. 4 XPS spectrum of ZnO nanorods deposited on Corning glass annealed at 600 °C in air ambient

mode of ZnO associated with oxygen deficiency. This weak intensity of the E_1 (LO) mode demonstrates that there is only limited oxygen vacancies in the ZnO nanorods. The red shift of the Raman spectrum in the nanostructures is usually related to phonon confinement effects caused by three factors the nano-dimension of the material, crystal defects, and lattice strains. The broadened Raman shifts from 1039 to 1184 cm^{-1} are known to be the vibration modes due to the multiple-phonon scattering process [21]. These results of the Raman spectrum imply that the prepared nanorods have low defects and strains.

During ultrasonication, a cavitation effect is usually noticed which plays a key role in the resulting nanostructures [22]. The ultrasonication not only provided the mechanical energy to dissolve the zinc precursor in the given solvent [23] but also induced molecular dispersion and micro-thermal effects in the system by which the formation of primary Zn^{2+} nuclei occurred in the reaction mixture. Such an initial nucleation stage is crucial for vertical and in-plane alignments of the nanorods. It is

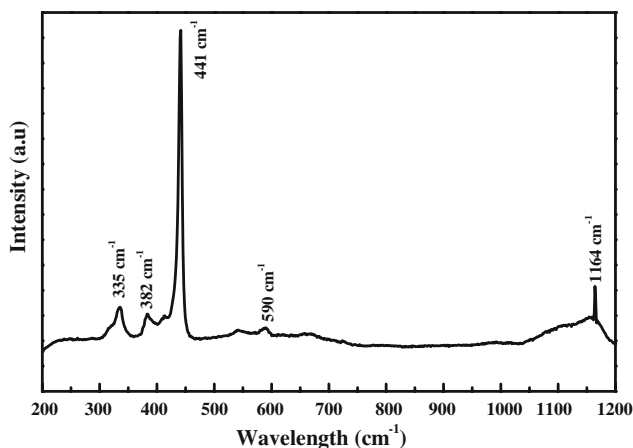
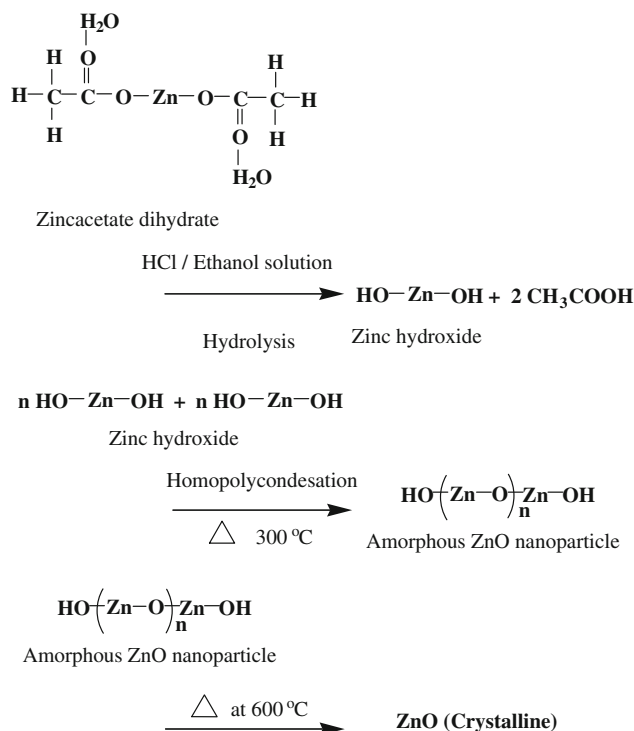


Fig. 5 Raman spectra of ZnO nanorods deposited on Corning glass annealed at 600 °C in air ambient

reasonable to mention that zinc ionic clusters deposited on the glass substrates serve as the nucleation centers for the growth of ZnO nanorods. The mechanism of ZnO nanorod assembly may be as follows: The zincacetate dihydrate is dissolved in ethanol and complete dissolution of the precursor is ensured by acid addition. Sonication induces the hydrolysis reaction in the presence of HCl/ethanol due to dissociation of ethanol and molecular-thermal heating. As a result, zinc hydroxide nuclei and acetic acid by-products are formed. When the sonicated precursor solution is spread over the glass substrate surface and subjected to heating at 300 °C, the ethanol evaporates rapidly but acetic acid leaves slowly. This results in homo-polycondensation to form semicrystalline ZnO nuclei. These grow to fully crystalline dense ZnO nanorods during annealing at 600 °C.



In our work, we have demonstrated the growth of ZnO nanorods in anhydrous ethanol medium at low pH without using any metallic catalysts. It appears that nanorod formation is most likely a self-catalytic process determined by the temperature and vapor pressures of Zn and oxygen. The pH value, sonication and initial reaction temperature (<60 degrees) are significant factors to be strictly controlled for forming the active seed layer as well as to achieve ZnO nanorod assembly.

4 Conclusions

We have presented a simple route to synthesize ZnO nanorods. Raman scattering indicates that the nanorods

have a hexagonal wurtzite phase with a fully crystalline quality with less structural defects. Ultrasonication appears to be advantageous for achieving active primary ZnO seed nuclei which favors oriented growth of ZnO nanorods. This procedure shows significant advantages when compared to other reported techniques especially in terms of simple processing equipments, low cost and that it can also be applied to large glass/polymer surfaces.

Acknowledgment This work was supported by the Center for Social Contribution and Collaboration (C-SoCC), Nagoya Institute of Technology, Japan.

References

1. Hunag MH, Mao S, Feick H, Yan JQ, Wu YY, Kind H, Webwe E, Russo R, Yang PD (2001) *Science* 292:1897. doi:[10.1126/science.1060367](https://doi.org/10.1126/science.1060367)
2. Pan ZW, Dai ZR, Wang ZL (2001) *Science* 291:1947. doi:[10.1126/science.1058120](https://doi.org/10.1126/science.1058120)
3. Samuelson L (2003) *Mater Today* 6:22. doi:[10.1016/S1369-7021\(03\)01026-5](https://doi.org/10.1016/S1369-7021(03)01026-5)
4. Lieber CM (2003) *MRS Bull* 28:486
5. Xia Y, Yang P, Sun Y, Wu Y, Mayers B, Gates B, Yin Y, Kim F, Yan H (2003) *Adv Mater* 15:353. doi:[10.1002/adma.200390087](https://doi.org/10.1002/adma.200390087)
6. Vayssieres L (2003) *Adv Mater* 15:464. doi:[10.1002/adma.200390108](https://doi.org/10.1002/adma.200390108)
7. Dev A, Kar S, Chakrabarti S, Chaudhuri S (2006) *Nanotechnology* 17:1533. doi:[10.1088/0957-4484/17/5/061](https://doi.org/10.1088/0957-4484/17/5/061)
8. Ohyama M, Kozuka H, Yoko T (1997) *Thin Solid Films* 306:78
9. Alfredom M, Leiber CM (1998) *Science* 279:208
10. Holmes JD, Johnston KP, Doty RC, Korgel BA (2000) *Science* 287:1471. doi:[10.1126/science.287.5457.1471](https://doi.org/10.1126/science.287.5457.1471)
11. Li Y, Meng GW, Zhang LD, Phillipp F (2000) *Appl Phys Lett* 76:2011. doi:[10.1063/1.126238](https://doi.org/10.1063/1.126238)
12. Kong X, Li Y (2003) *Chem Lett* 32:838. doi:[10.1246/cl.2003.838](https://doi.org/10.1246/cl.2003.838)
13. Zhang X, Zhao H, Tao X, Zhao Y, Zhang Z (2005) *Mater Lett* 59:1745. doi:[10.1016/j.matlet.2005.01.046](https://doi.org/10.1016/j.matlet.2005.01.046)
14. Suslick KS, Price GJ (1999) *J Ann Rev Mater Sci* 29:295
15. Pol VG, Reisfeld R, Gedanken A (2002) *Chem Mater* 14:3920. doi:[10.1021/cm0203464](https://doi.org/10.1021/cm0203464)
16. Cheng B, Edward TS (2004) *Chem Commun (Camb)* 2:986. doi:[10.1039/b316435g](https://doi.org/10.1039/b316435g)
17. Cao HL, Qian XF, Gong Q, DU WM, Ma XD, Zhu ZK (2006) *Nanotechnology* 17:3632. doi:[10.1088/0957-4484/17/15/002](https://doi.org/10.1088/0957-4484/17/15/002)
18. Jung SH, Oh E, Lee KH, Park W, Jeong SH (2007) *Adv Mater* 19:749. doi:[10.1002/adma.200601859](https://doi.org/10.1002/adma.200601859)
19. Ghoshal T, Kar S, Chaudhuri S (2006) *J Cryst Growth* 193:438. doi:[10.1016/j.jcrysgro.2006.06.002](https://doi.org/10.1016/j.jcrysgro.2006.06.002)
20. Wang M, Ye C-H, Zhang Y, Hua G-M, Wang H-X, Kong M-G, Zhang L-D (2006) *J Cryst Growth* 291:334. doi:[10.1016/j.jcrysgro.2006.03.033](https://doi.org/10.1016/j.jcrysgro.2006.03.033)
21. Chen BJ, Sun XW, Xu CX, Tay BK (2004) *Physica E* 21:103. doi:[10.1016/j.physe.2003.08.077](https://doi.org/10.1016/j.physe.2003.08.077)
22. Jung SH, Oh E, Lee KH, Jeong SH, Yang Y, Park CG (2007) *Bull Korean Chem Soc* 28(9):1457
23. Sivakumar M, Towata A, Yasui K, Tuziuti T, Iida Y (2006) *Chem Lett* 35:60. doi:[10.1246/cl.2006.60](https://doi.org/10.1246/cl.2006.60)